

for his many useful comments and motivation, and W. P. Halperin for providing us with his unpublished He³ melting curve.

¹D. D. Osheroff, Ph.D. thesis, Cornell University, 1972 (unpublished).

²W. J. Gully, D. D. Osheroff, D. T. Lawson, R. C. Richardson, and D. M. Lee, Phys. Rev. A 8, 1633 (1973).

³V. Ambegaokar and N. D. Mermin, Phys. Rev. Lett. 30, 81 (1973).

⁴C. M. Varma and N. R. Werthamer, Bull. Amer. Phys. Soc. 18, 23 (1973). These authors considered only the low-field limit and hence predicted only two transitions.

⁵W. F. Brinkman and P. W. Anderson, Phys. Rev. A 8, 2732 (1973).

⁶P. W. Anderson and W. F. Brinkman, Phys. Rev.

Lett. 30, 1108 (1973).

⁷P. W. Anderson and P. Morel, Phys. Rev. 123, 1911 (1961).

⁸W. F. Brinkman, J. W. Serene, and P. W. Anderson, to be published. A calculation along similar lines by Y. Kuroda (to be published) gives results which agree with BSA for the purpose of this paper.

⁹A. J. Leggett, Phys. Rev. Lett. 31, 352 (1973), and Ann. Phys. (New York) 85, 11 (1974).

¹⁰Since the submission of this work for publication we have received a preprint of an article by S. Takagi (to be published) which also derives the frequency shift in A₁ for a more general class of states and arrives at the same result.

¹¹J. C. Wheatley, Physica (Utrecht) 69, 218 (1973).

¹²D. D. Osheroff and W. F. Brinkman, Phys. Rev. Lett. 32, 584 (1974).

¹³W. P. Halperin, private communication.

¹⁴R. Balian and N. R. Werthamer, Phys. Rev. 131, 1553 (1963).

Ion Heating by an Intense Relativistic Electron Beam

J. P. VanDevender, J. D. Kilkenny, and A. E. Dangor

Imperial College, London SW7 2BZ, England

(Received 24 July 1974)

A high-current electron beam is used to produce a plasma from neutral hydrogen. Doppler-line-broadening and Thomson-scattering measurements show that the ion energy is 100 ± 15 eV compared with only 12 ± 2 eV for the electron energy. It is shown that this ion energy can be supplied by an inverse pinch effect. It is suggested that much higher ion energies will result for electron densities n_e lower than 10^{15} cm⁻³ measured here.

Several experimenters¹⁻⁷ have reported that when a high-current relativistic electron beam is injected into a plasma, a fraction of the beam energy is transferred to the plasma through the excitation of streaming instabilities. The energy is transferred primarily to the plasma electrons. In this paper we report measurements which show that direct energy transfer to the ions can occur if the self-magnetic field of the beam is not completely neutralized by the counter-streaming plasma current—for, in such a situation, there exists a force $\vec{j} \times \vec{B}$, associated with the plasma current and the magnetic field due to the net current, which accelerates the plasma radially outward. This is the main force acting on the plasma since the coupling between the beam and plasma electrons is weak. The energy for the radial motion is of course provided by the beam.

The experimental arrangement is shown in Fig. 1. A 36-kA, 350-kV, 100-nsec electron beam is

compressed by a cone to a current density of 20 kA/cm² and injected through a Mylar foil into a test chamber, which is filled with neutral hydrogen. There is no external magnetic field. The current and energy of the beam are reproducible

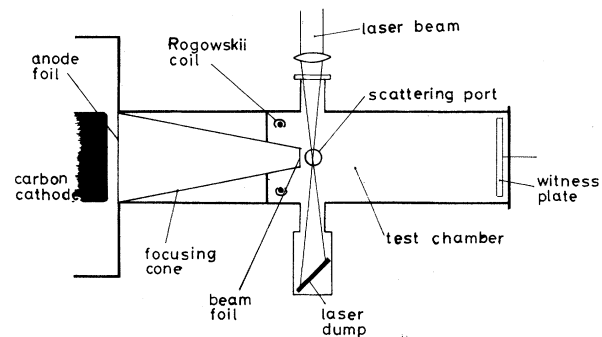


FIG. 1. Diagram of the apparatus. The line-broadening measurements are made by using the laser scattering ports.

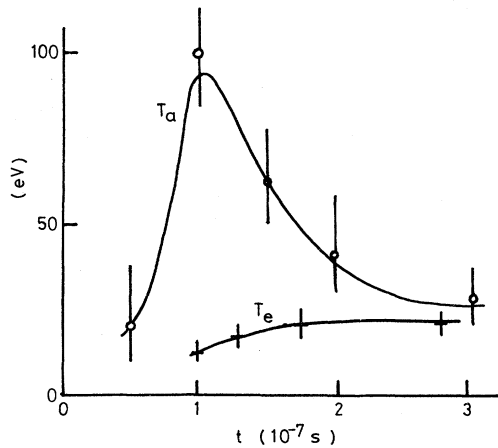


FIG. 2. Electron temperature (T_e) from Thomson scattering. Effective atom temperature (T_a) from Doppler broadening of the Balmer lines by both macroscopic and microscopic motion. Injection is into 100-mTorr H_2 and time is relative to the start of the beam.

to within 10%. The beam radius r_b , measured by the damage pattern on a witness plate, is 8 ± 1 mm throughout the test chamber. The plasma produced by the beam is diagnosed by (1) line broadening of the hydrogen Balmer lines along a line of sight perpendicular to the beam, (2) ruby-laser scattering with the scattering vector also perpendicular to the beam, (3) streak photography, and (4) the net current $I_{net} = I_{beam} - I_{plasma}$, measured with the Rogowski coil shown in Fig. 1. Measurements (1), (2), and (3) are made 8 mm from the entrance foil.

There are two contributions to the line widths: Stark and Doppler broadening. The tabulated Stark broadening of H_β is an order of magnitude larger than for H_α .⁸ Experimentally it is found that the widths of the two lines are comparable. Thus the atom velocity distribution along the line of sight can be obtained by analysis of the line widths.⁹ The average energy per atom deduced from the data is shown in Fig. 2, for injection into 100-mTorr hydrogen. The charge-exchange mean free path for H^+ in 100-mTorr H_2 is typically 1 mm and so the atom energy is a measure of the ion energy.

Also shown in Fig. 2 is the electron energy obtained from the laser-scattering measurements. Note that at the end of the electron-beam pulse the plasma-electron energy is 12 eV, an order of magnitude less than the atom and ion energy.

Figure 3 is a streak photograph of the diameter of the plasma channel for injection into 100-

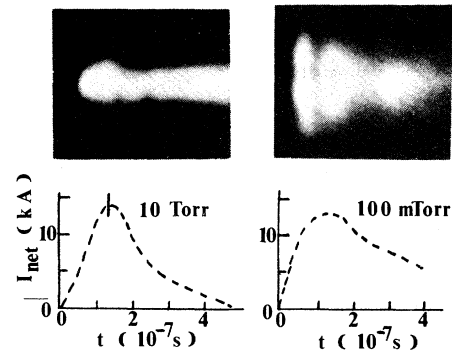


FIG. 3. Streak photograph of a plasma diameter contrasting injection into 100-mTorr H_2 where the radius of the plasma channel changes, with 10-Torr H_2 where the radius is approximately constant.

mTorr and 10-Torr neutral hydrogen. For the 10-Torr case the diameter of the channel is approximately constant. At 100 mTorr the plasma is first seen expanding at 100 nsec, reaching its maximum radius of 2 cm, twice that of the electron beam, at 130 nsec. The initial light at the walls is due to electrons which are expelled from the plasma to give charge neutralization. After the beam the plasma pinches to the axis.

The net currents for 10 Torr and 100 mTorr are shown in Fig. 3. At both pressures the net current is found to start decaying at a time later than 100 nsec, the beam pulse length. In general, it is found that the net current continues to increase for a longer time and that the net change is greater as the pressure is reduced.

The continuum plasma light emission is shown in Fig. 4 together with the plasma current I_{plasma} . For injection into hydrogen at pressures greater than 100 mTorr the light emission follows the plasma current. However at lower pressures, the light emission drops quickly during the beam pulse.

The results presented above—(1) the Doppler broadening, (2) the size of the plasma at 130 nsec, (3) the increase of the net current after the beam, and (4) the absence of light emission during the beam pulse at low pressure—are consistent with radial motion of the plasma. The pinching observed after the beam pulse suggests that the radial motion is associated with the force $j_z B_\theta$ on the plasma.

During the beam pulse the plasma current j_{pz} is opposite in direction to the net current, which produces the azimuthal field B_θ . Thus during the beam, the force is radially outward. After the

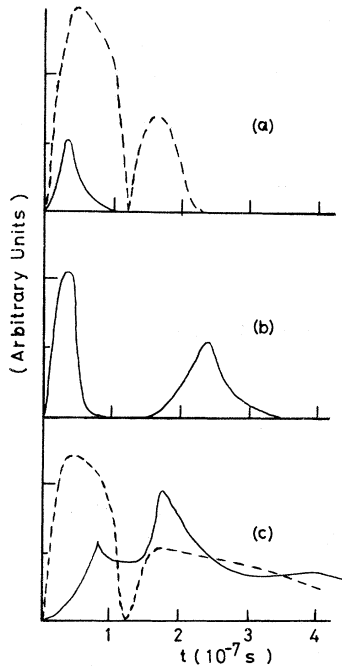


FIG. 4. Time history of the continuum light emission near 6940 Å (solid line) and the modulus of the plasma current (broken line) in arbitrary units. (a) 2 mTorr, (b) 30 mTorr, (c) 60 mTorr. Notice the correlation at 60 mTorr and contrast the rapid drop in plasma light at lower pressure.

beam the only current in the system is the plasma current and therefore, the plasma pinches. A measure of the radial acceleration can be obtained from the equation of motion

$$\rho dv_r/dt = -j_{pz} B_\theta. \quad (1)$$

Taking ρ as the mass density of the neutral gas, j_{pz} the plasma current density as $(I_{net} - I_{beam})/\pi r_b^2$, and B_θ equal to $\frac{1}{2}$ the maximum value at the beam radius, we obtain the equation $dv_r/dt \sim 10^{12}$ m sec $^{-2}$. Thus in 100 nsec, a velocity v_r of 10^5 m sec $^{-1}$ and a plasma expansion of 1 cm are expected. This is in agreement with the measured Doppler velocity of 1.3×10^5 m sec $^{-1}$ and the observed radius of the plasma.

After the beam pulse the plasma current reverses, and the force $\vec{j} \times \vec{B}$ on the plasma is radially inward. For a plasma of zero resistivity the sum of the magnetic ($\frac{1}{2}LI_{net}^2$) and kinetic energies is then constant. As the plasma is decelerated the energy in the mass motion is transferred to field energy so that at the end of the pulse and be-

fore the plasma motion is reversed,

$$\frac{dI_{net}}{dt} > -\frac{1}{2} \frac{I_{net}}{L} \frac{dL}{dt}.$$

Since the channel is still expanding dL/dt is negative and so dI_{net}/dt is positive, in agreement with the net-current measurements.

As the force $\vec{j} \times \vec{B}$ on the plasma expels the plasma from the channel the plasma number density within the channel drops if additional ionization cannot compensate. This is consistent with the drop in light emission from the plasma during the beam pulse at very low pressures.

The effect is important because of the energy transfer from an electron beam to the ions in a plasma. Consider an infinitely long system. The axial component of Ohm's law is

$$\eta j_{pz} = E_z + v_r B$$

provided $\text{div} \vec{j} = 0$. The rate of increase of the plasma energy density is $j_{pz} E_z$ of which ηj_{pz}^2 is the resistive heating and $-v_r B_\theta j_{pz}$ is the rate of energy transfer to the heavy particles. According to Eq. (1) the acceleration dv_r/dt is proportional to ρ^{-1} . Thus at lower filling pressures, the energy input to the ions will dominate the electron heating even more than it does for this experiment at $n_e = 10^{15}$ cm $^{-3}$. An approximate calculation shows that ion viscosity can easily randomize this energy.

In summary, measurements of a plasma produced by an electron beam in neutral hydrogen have shown that the neutral and ion energies are an order of magnitude greater than the electron energy. This new result has not been observed before as most other experiments have been performed with a much larger mass density. We have not examined the role of a guide field, and also this effect depends on incomplete magnetic neutralization. However, the injection of a beam along a z -pinch column, which has a significant B_θ , would produce this energy transfer mechanism.

We wish to thank J. C. Martin and his associates at the Atomic Weapons Research Establishment, Aldermaston, England, for their help with the electron-beam technology, and the loan of a Marx generator. Our thanks are also due to J. A. Nation and J. Westlake for advice and assistance.

¹A. T. Altyntsev *et al.*, Nucl. Fusion, Suppl., 161 (1972).

²D. R. Smith, Phys. Lett. **42A**, 211 (1972).

³C. A. Kapetanacos and D. A. Hammer, Appl. Phys. Lett. **23**, 17 (1973).

⁴P. A. Miller and G. W. Kuswa, Phys. Rev. Lett. **30**, 958 (1973).

⁵P. Korn, F. Sandel, and C. B. Wharton, Phys. Rev. Lett. **31**, 579 (1973).

⁶G. C. Goldenbaum, W. F. Dove, K. A. Gerber, and B. G. Logan, Phys. Rev. Lett. **32**, 830 (1974).

⁷C. Stallings, D. Prono, R. Schneider, and S. Putnam, Bull. Amer. Phys. Soc. **18**, 1350 (1973).

⁸H. R. Griem, *Plasma Spectroscopy* (McGraw-Hill, New York, 1964).

⁹J. D. Kilkenny, unpublished.

Dissipative Trapped-Electron Instability in Cylindrical Geometry*

S. C. Prager, A. K. Sen, and T. C. Marshall

Plasma Research Laboratory, Columbia University, New York, New York 10027

(Received 28 May 1974)

We show that the essential ingredients of the trapped-electron instability can be present in a cylindrical geometry. A linear instability theory, a simple physical explanation, and the results of an experiment are presented to support this.

The dissipative trapped-electron instability like all other trapped-particle instabilities has always been discussed in toroidal systems.¹⁻³ In toroidal systems magnetic field properties such as inhomogeneity, curvature, and helicity are all interrelated and the resulting zero-order particle trajectories of drifting bananas are very complex. These geometrical complexities also make experimental identification difficult. This Letter considers the simplest magnetic field sufficient for the instability and clarifies the underlying physics. We also report the results of an experiment which demonstrates that a dissipative trapped-electron instability can be excited in a cylindrical geometry.

It is well known that collisionless trapped-particle instabilities are driven by magnetic-curvature drift.³ But dissipative trapped-particle instabilities are similar to collisional drift waves in the sense that the excitation of both classes depends on collisions. In the case of the trapped-electron instability one needs an appropriate electron collision frequency which should be higher than the wave frequency.¹ Therefore one can conceive of the dissipative trapped-electron instability in an essentially straight magnetic field, but to produce a trapped population of particles one needs at least two localized magnetic

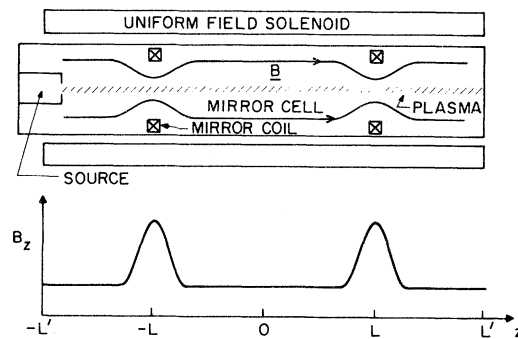


FIG. 1. Schematic of the mirror cell in cylindrical geometry (above) and the axial magnetic field intensity (below) for mirror ratio $R=3$. The plasma source which produces a radial electron-temperature gradient is an $\vec{E} \times \vec{B}$ source (Ref. 5).

mirrors (Fig. 1). A density gradient, say in the radial direction, is always necessary for a drift-like mode and finally, an electron-temperature gradient coincident with the density gradient is essential.¹ We will show that the cylindrical system shown in Fig. 1 is capable of sustaining the dissipative trapped-electron instability.

For electrons trapped between the mirrors, we write the drift kinetic equation in cylindrical coordinates r, θ, z with the Krook model for the collision term as

$$\frac{\partial f_t}{\partial t} + v_z \frac{\partial f_t}{\partial z} + \frac{e}{m_e} \frac{\partial \varphi}{\partial z} \frac{\partial F_t}{\partial v_z} - \frac{c}{B_z r} \frac{\partial \varphi}{\partial \theta} \frac{\partial F_t}{\partial r} = \nu_e(v) \left(\frac{e \varphi}{k T_e} F_t - f_t \right), \quad (1)$$

where f and φ are the perturbed electron distribution function and potential, respectively; v_z , $\nu_e(v)$, and F are the axial velocity, velocity-dependent electron collision frequency, and equilibrium distribu-

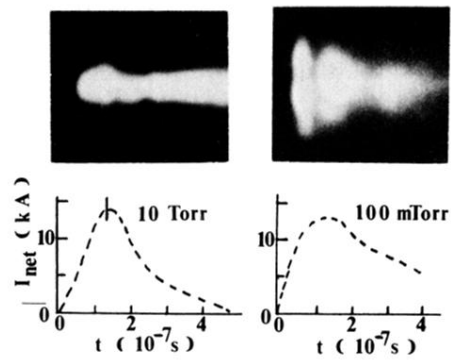


FIG. 3. Streak photograph of a plasma diameter contrasting injection into 100-mTorr H_2 where the radius of the plasma channel changes, with 10-Torr H_2 where the radius is approximately constant.